

Resonant energy transfer from silicon nanocrystals to iodine moleculesToshihiro Nakamura,* Tatsuya Ogawa, and Sadao Adachi
Graduate School of Engineering, Gunma University, Kiryu, Gunma 376-8515, Japan

Minoru Fujii

Department of Electrical and Electronics Engineering, Faculty of Engineering, Kobe University, Rokkodai, Nada, Kobe 657-8501, Japan

(Received 10 June 2008; published 10 February 2009)

The electronic excitation energy transfer between excitons in silicon nanocrystal assemblies and iodine molecules in an organic solution is studied. From the time-resolved photoluminescence the rate of the energy transfer is found to increase with approaching a wavelength region, where the photoluminescence spectrum of nanocrystals overlaps the absorption spectrum of iodine molecules, and with increasing the radiative recombination rate of nanocrystals. The energy-transfer rate is also found to depend on the concentration of iodine molecules. This dependence is well explained by Förster-type dipole-dipole interaction mechanism in which the diffusion of the assemblies and molecules is taken into consideration.

DOI: [10.1103/PhysRevB.79.075309](https://doi.org/10.1103/PhysRevB.79.075309)

PACS number(s): 78.67.Bf, 33.50.Hv, 71.35.Gg, 78.47.Cd

I. INTRODUCTION

Silicon (Si) nanocrystal is a promising material for optoelectronic devices because of its strong visible and near infrared photoluminescence (PL) at room temperature. The efficient luminescence is due to the recombination of quantum confined excitons.¹⁻³ The typical system which contains luminescent Si nanocrystal assemblies is porous Si. Because porous Si is easily prepared by the anodic electrochemical etching in a HF-based solution and has high luminescent efficiency, the structural and optical properties of porous Si have been intensively investigated.⁴

The radiative lifetime of exciton in Si nanocrystal is rather long (approximately microsecond range) because of the inheritance of indirect band-gap nature of bulk Si. Then, it is difficult to realize the light emitting devices based on the Si nanocrystal assemblies, although the improvement of the emission quantum efficiency can be achieved by various methods such as a uniform surface passivation to suppress the influence of surface defects.⁵ It has been demonstrated that Si nanocrystals can be used as an efficient photosensitizer for rare-earth ions^{6,7} and molecular oxygen.⁸ Particularly, in the photosensitizing effect for the molecular oxygen, the long lifetime of exciton in Si nanocrystal plays an important role since the decay time of excitons is longer than the transfer time of electronic excitation energy to molecular oxygen. The large surface area in Si nanocrystal assemblies is also an advantage for the energy transfer.

Si nanocrystals can be used as a photosensitizer for other materials such as organic molecules. Recently, the energy transfer from Si nanocrystals to organic molecules is demonstrated.⁹ In that work, the energy transfer takes place via direct electron exchange interaction called Dexter process, which is the same mechanism as that between Si nanocrystals and molecular oxygen. Basically, the electronic excitation energy of donor can nonradiatively transfer to acceptor via dipole-dipole Coulombic interaction called Förster process,¹⁰ together with Dexter process. In colloidal semiconductor nanocrystals such as CdSe quantum dots, the excitation energy transfer to organic dye molecules or nearby

quantum dots via Förster process is observed.^{11,12} Therefore, Si nanocrystals can be expected for use as the energy donor in Förster-type energy transfer. It is important to investigate Förster process in Si nanocrystals. This is because Si nanocrystals have a longer lifetime compared to direct band-gap semiconductor quantum dots and exhibit the size tunable PL spectra allowing the excitation of an acceptor at a suitable wavelength and the broad absorption band in an ultraviolet region. However, there are a few works on the process in Si nanocrystals.¹³

In this work we demonstrate that the excitation energy of the Si nanocrystal assemblies transfers to acceptor molecules via Förster-type dipole-dipole interaction in an organic solution. To reveal that Si nanocrystals act as the energy donor in this type of resonant energy transfer, the analysis of PL spectral changes in Si nanocrystals in the presence of any acceptor molecules is needed because the energy transfer accompanies the resonant quenching of PL intensity of donor.⁹ Therefore, we should choose a molecule which does not emit light near the PL band of Si nanocrystals as an energy acceptor. Here, iodine molecules are used as the acceptor because of its small influence on the PL of Si nanocrystals due to its low intrinsic dipole moment and a large spectral overlap between absorption of iodine and PL of Si nanocrystals.¹³ The combination between the iodine molecules and Si nanocrystals is a typical system to make clear that the Si nanocrystals can act as an efficient donor in Förster-type energy-transfer process. We show that the rate of energy transfer strongly depends on the emission wavelength, i.e., the size of Si nanocrystals. Furthermore, we show that the dependence of the energy-transfer rate on the concentration of iodine molecules is well explained by Förster model.

II. EXPERIMENTAL PROCEDURE

We used porous Si powder as a nanocrystal assembly. The porous Si was prepared by a stain-etching process.¹⁴ Metallurgical-grade polycrystalline Si powder (Vesta Ceramics, with mean diameter of 3–11 μm) was immersed in an

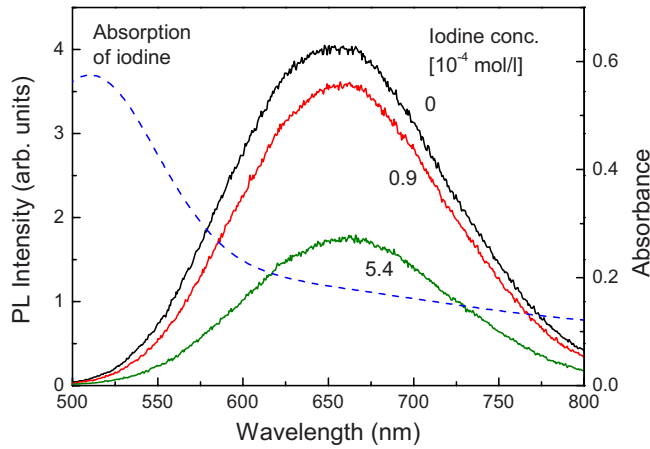


FIG. 1. (Color online) PL spectra of a porous Si powder dispersed in trichloroethylene with adding iodine molecules. The concentration of iodine solutions is varied from 0 to 5.4×10^{-4} mol/l. The dashed line represents an absorption spectrum of iodine molecules (right axis).

aqueous HF solution and then gradually added HNO_3 in it with final concentration of $\text{HF}:\text{HNO}_3:\text{H}_2\text{O}=4:1:20$ for 20 min. After etching, the powder was collected from the etching solution and dried at ambient condition for 24 h. The etched powder shows efficient orange emission by exciting with ultraviolet light. The Fourier-transform infrared spectroscopy (FT-IR) measurement suggested that the as-prepared powder shows the absorption peak at around 2090 cm^{-1} which corresponds to the Si-H_2 stretching mode. This indicates that the porous Si powder prepared has H-terminated surface.

For PL measurement, porous Si powder was dispersed in trichloroethylene with a quartz cell. Iodine molecules were gradually mixed in trichloroethylene solution at final concentration of 5.4×10^{-4} mol/l. During optical measurements, the solution was permanently mixed using a magnetic stirrer.

The excitation source for PL measurements was 355 nm light from the third harmonic of a Nd:yttrium aluminum garnet (YAG) laser (pulse width of 5 ns and repetition frequency of 20 Hz). The time-integrated and time-resolved PL spectra were measured by a spectrometer equipped with a gated charge coupled device (PI-Max, Princeton Instrument, 5 ns response time). In a time-resolved PL measurement the delay time after excitation pulse was set to be 20 ns with a gate width of 60 ns. All measurements were performed at room temperature.

III. RESULTS AND DISCUSSION

Figure 1 shows time-integrated PL spectra of porous Si powder dispersed in a trichloroethylene containing iodine molecules (solid line, left axis). The concentration of iodine is varied from 0 to 5.4×10^{-4} mol/l. The PL intensity decreases with increasing the iodine concentration and the peak wavelength slightly shifts to longer wavelength region. The absorption spectrum of iodine solution is also shown in Fig. 1 (dashed line, right axis). An absorption band at around 500 nm is seen. The visible-infrared-absorption band of iodine

corresponds to the mixing of three electronic transitions, $1u(^1\Pi) \leftarrow X[O^+g(^1\Sigma)]$, $B[O^+u(^3\Sigma)] \leftarrow X$, and $A[1u(^3\Pi)] \leftarrow X$.¹⁵ The ultraviolet absorption band of iodine due to $D[O^+u(^1\Sigma)] \leftarrow X$ electronic transition is located at around 280 nm (Ref. 16) and the tail of its band slightly overlaps the 355 nm YAG:Nd line. It is also found that the PL spectrum of porous Si overlaps the absorption spectrum of iodine molecules very well in the range from 500 to 600 nm.

The PL quenching is also observed in chloroform and toluene but not in acetone. For chloroform and toluene, visible absorption peaks are almost the same as for trichloroethylene and the spectral overlap with the porous Si PL is very large. In the case of acetone the peak of the absorption occurs at much shorter wavelength (around 380 nm) and it does not overlap PL of porous Si. The observed PL quenching that depends on the degree of the spectral overlap suggests that the quenching arises from radiative or nonradiative resonant energy transfer to iodine molecules.

The time-resolved PL spectra of porous Si powder dispersed in the solutions without (solid lines) and with iodine molecules at 5.4×10^{-4} mol/l (dashed lines) are shown in Fig. 2(a). The gate width in PL measurements was 60 ns, and the delay time with respect to the excitation pulse was varied from 0.02 to 6 μs . The PL intensity is quenched by adding the iodine molecules, and the degree of the quenching becomes larger as the delay time increases and emission wavelength approaches the absorption peak of iodine molecules (vertical dashed line). The PL decay curves of porous Si powder for various iodine concentrations detected at 567 nm (open square) and 700 nm (closed square) are plotted in Fig. 2(b). As the iodine concentration is increased, the lifetime becomes shorter. The lifetime shortening depends on the emission wavelength. While the PL decay curve in the 1.6×10^{-4} mol/l iodine solution detected at 700 nm is almost the same as that without iodine, these curves detected at 567 nm are quite different.

Let us consider several reasons for the PL quenching and shortening of lifetime. Fojtik and Henglein¹⁷ reported the quenching of colloidal Si particles by adding the polar solvents, triethylamine, and sulfuric acid. They concluded that the quenching mechanism is due to a change in the surface charges, i.e., the protonization state change in a luminescence center. This mechanism may also occur in our iodine-contained solutions. According to the literature,¹⁸ the protonization quenching process is considered to be a static phenomenon and thus the lifetime is essentially unchanged. In our case, the PL quenching is clearly a dynamic process because the lifetime shortening simultaneously occurred; therefore, the protonization quenching effects do not occur.

Fojtik and Henglein¹⁹ also found that the luminescence is quenched by attacking their surfaces by free radical which is generated by exposing γ radiation. The quenching is caused by dissolving the silicon or destroying the luminescence centers. To confirm the effect, we performed photostability measurement by laser irradiation but not observed a PL quenching or lifetime change. Therefore, we can exclude the possibility of nanocrystalline clusterization by direct laser irradiation and attack of the radical generated by the laser irradiation.

Changes in the porous Si surface by adding iodine are possible mechanisms of PL quenching. To investigate the ef-

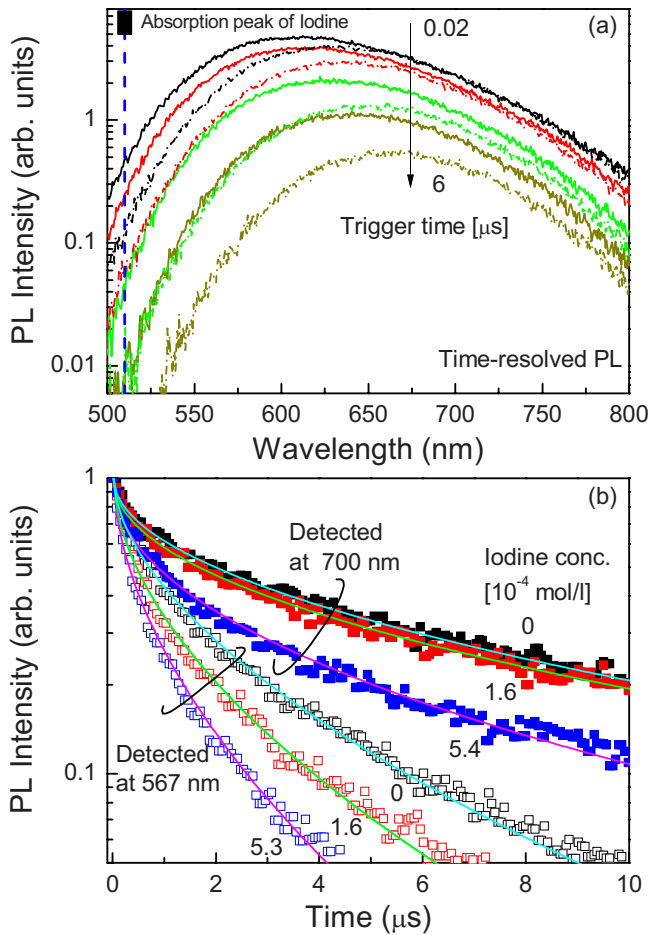


FIG. 2. (Color online) (a) Time-resolved PL spectra of a porous Si powder dispersed in trichloroethylene with (dashed lines) and without adding iodine molecules (solid lines). The gate time is 60 ns. The data taken with various delay time from the excitation pulse of 0.08, 0.3, 2, and 6 μs are shown. The absorption peak wavelength of iodine molecule is shown by the vertical dashed line. (b) PL decay curves detected at 567 nm (open symbols) and at 700 nm (closed symbols). The concentration of iodine molecules is varied from 0 to 5.4×10^{-4} mol/l.

fect of surface termination, we performed x-ray photoelectron spectroscopy (XPS) and FT-IR measurements for dried porous silicon samples before and after immersing the samples in the iodine-contained solution. From XPS and FT-IR measurements, we cannot observe significant change in the surface states related Si atom. These results suggest that the surface chemistry is unchanged so largely before and after iodine immersion.

From the above facts the shortening of lifetime accompanied by the PL quenching is consider to be due to the non-radiative energy transfer from excitons confined in Si nanocrystals to iodine molecules. The spectral dependence of the energy-transfer intensity is obtained by dividing the time transient of the PL intensity of porous Si with iodine (I_w) by that without iodine (I_{w0}) measured under the same gate duration and delay time.²⁰ Figure 3 shows plots of I_w/I_{w0} versus wavelength for iodine concentrations (a) 0.4×10^{-4} , (b) 1.6×10^{-4} , and (c) 5.4×10^{-4} mol/l. In low iodine concentration [Fig. 3(a)], the spectra are slightly changed in the

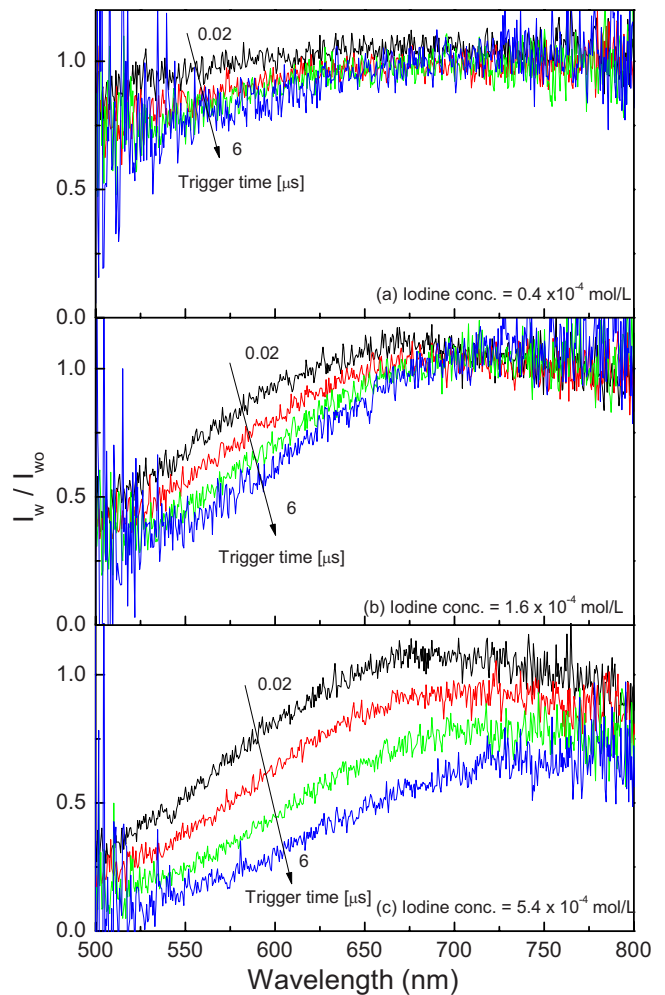


FIG. 3. (Color online) Time-resolved PL spectra of a porous Si powder in trichloroethylene with adding iodine molecules divided by the PL strengths without adding iodine (I_w/I_{w0}). The gate time is 60 ns. The data taken with various delay time from the excitation pulse of 0.08, 0.3, 2, and 6 μs are shown. The concentrations of iodine solutions are (a) 0.4×10^{-4} , (b) 1.6×10^{-4} , and (c) 5.4×10^{-4} mol/l.

range from 500 to 600 nm with time delay. In longer wavelength region no clear change is observed ($I_w/I_{w0}=1$). The same tendency is observed in the middle iodine concentration [Fig. 3(b)] with more dramatic change in the spectral shape at shorter wavelength region. In high iodine concentration [Fig. 3(c)], the spectral shape is changed largely with delay time. In addition I_w/I_{w0} is decreased over the whole wavelength region especially with increasing delay time.

The above results suggest that the energy transfer from excitons to iodine molecules efficiently occurs resonantly, that is, when the band-gap energy of porous Si coincides with the energy of electronic state of iodine molecules. Moreover, the rate of energy transfer strongly depends on the iodine concentration, i.e., the number of iodine molecules surrounding Si nanocrystals. It should be noted, however, that in the highest iodine concentration the energy transfer occurs under the nonresonant condition [spectral overlap between the PL band of porous Si and the absorption of iodine

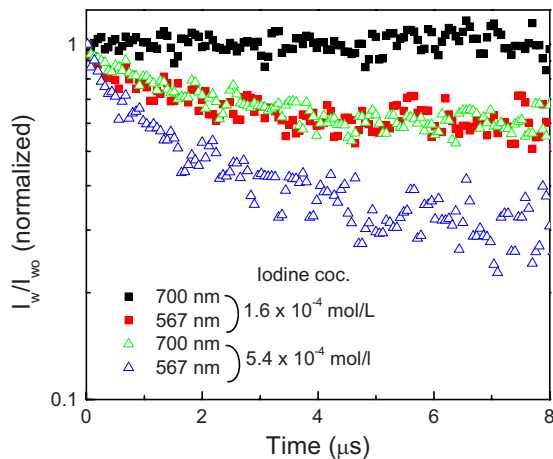


FIG. 4. (Color online) I_w/I_{w0} as a function of delay time detected at 567 and 700 nm. The concentrations of iodine solutions are 1.6×10^{-4} (closed squares) and 5.4×10^{-4} (open triangles) mol/l.

is relatively small in the range from 600 to 800 nm (see Fig. 1)].

Figure 4 shows the delay-time dependence of I_w/I_{w0} normalized to 1 at $0.02 \mu\text{s}$. The iodine concentrations are 1.6×10^{-4} and 5.4×10^{-4} mol/l. It is clearly seen that the I_w/I_{w0} curve detected at 567 nm is more abruptly decreasing than that detected at 700 nm for both concentrations. Because their slope corresponds to energy-transfer time,²⁰ the energy-transfer time at 567 nm is determined to be shorter than that at 700 nm. Moreover, the energy-transfer time depends on the iodine concentration, and its values at 576 nm are 1.57 and $1.9 \mu\text{s}$ for 5.4×10^{-4} and 1.6×10^{-4} mol/l, respectively. The wavelength dependence of the transfer time indicates that the energy transfer resonantly occurs as mentioned above.

When iodine molecules exist in the solution dispersed with porous Si powders, additional decay channels for the excitons in Si nanocrystals may be introduced due to the energy transfer to the iodine molecules. The introduction of the additional channels results in the enhancement of the decay rate (shortening of the lifetime). To discuss quantitatively, the decay rate is determined by fitting the PL transient curves of porous Si with an exponential function. In Fig. 2(b) examples of these fits are shown by solid lines. We can see that the curves are well fitted. Figure 5(a) shows estimated decay rates of porous Si in solutions of various iodine concentrations as a function of the emission wavelength. The increase in the decay rate in the shorter wavelength region is observed. This is due to a larger overlap of the electron and hole wave functions in a momentum space by the quantum confinement effect.²¹ Decay rates at 1.6×10^{-4} mol/l iodine concentration are larger than those without iodine molecules in the range from 500 to 650 nm. At 5.4×10^{-4} mol/l iodine concentration, decay rates are enhanced in the whole wavelength range. These enhancements provide clear evidence of the nonradiative energy transfer from porous Si to iodine molecules.

In the presence of iodine molecules in the solution dispersed with porous Si powders the decay rate of excitons

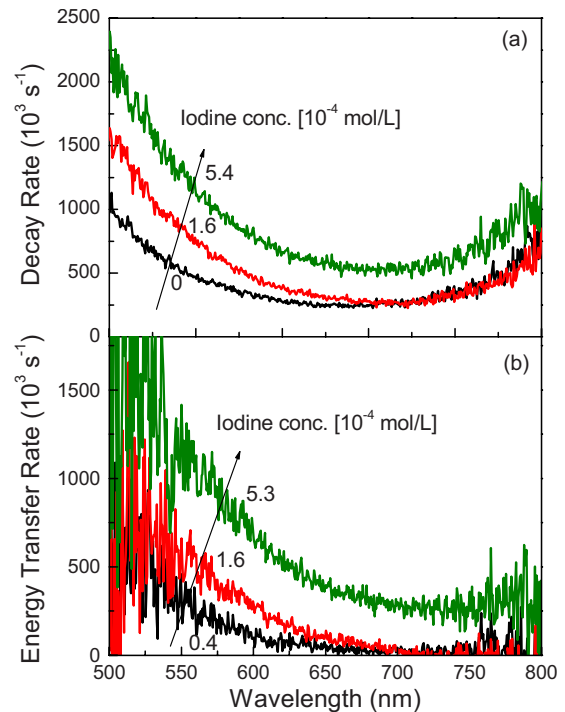


FIG. 5. (Color online) (a) PL decay rate of porous Si dispersed in a solution with iodine molecules as a function of the emission wavelength. The concentrations of iodine solutions are 0, 1.6×10^{-4} , and 5.4×10^{-4} mol/l. (b) Energy-transfer rate as a function of emission wavelength. The concentrations of iodine solutions are 0.4×10^{-4} , 1.6×10^{-4} , and 5.4×10^{-4} mol/l.

measured from PL decay curves consists of the three components, the radiative recombination rate k_r , the nonradiative one k_{nr} , and the energy transfer to the iodine k_{et} . If an increase in the decay rate in the presence of iodine molecules is caused only by the energy transfer, its energy-transfer rate can be estimated by subtracting the decay rate without iodine ($k_r + k_{nr}$) from that with iodine ($k_r + k_{nr} + k_{et}$). In Fig. 5(b), the energy-transfer rate estimated from this procedure is plotted as a function of emission wavelength. As shown in Fig. 5(b) the energy-transfer rate strongly depends both on the emission wavelength and iodine concentration. The energy-transfer rates are increased to shorter wavelength side for all iodine concentrations. At low iodine concentrations, the increase in the rate is observed with decreasing wavelength in the range from 650 to 500 nm, and at >650 nm the rates are nearly zero, i.e., the energy transfer does not occur. In contrast, at the highest concentration the rate starts to increase at 700 nm and the energy transfer takes place over the whole wavelength range.

A possible mechanism of the nonradiative energy transfer from excitons formed in the porous Si to iodine molecules accounts for the Förster-type dipole-dipole interaction.¹³ The rate of Förster-type energy transfer depends on the dipole oscillator strength in donor and acceptor and the distance between donor and acceptor.¹⁰ From the Förster theory for energy transfer in a single donor-acceptor pair, the rate of energy transfer k_{et} can be given by $k_{et} = k_r (r/R_0)^{-6}$, where R_0 is the Förster distance in which the transfer is 50% efficient, k_r is the decay rate of a donor, and r is the distance between

a donor and an acceptor. In our case, the energy transfer occurs from donors (excitons in Si nanocrystals) to acceptors (iodine molecules); those are randomly distributed in a solution. Therefore, we should take the situation into account for the calculation of the energy-transfer rate. In addition, the diffusion of donors and acceptors may affect the rate of energy transfer because the lifetime of excitons (microseconds) is much longer than that of typical fluorescent organic molecules.²² To consider these conditions we assume that the rapid-diffusion limit^{23,24} is attained in our energy-transfer system. It is adopted in a system where the mean distance diffused by donor and acceptor is sufficiently smaller than the diffusion distance during the lifetime of donor. The energy-transfer rate in this limit is

$$k_{\text{et}} = 4\pi\rho R_0^6 k_r / 3a^3, \quad (1)$$

where a and ρ are the closest approached distance between donor and acceptor and the density of acceptor, respectively.

To check the validity of this assumption, we try to fit the acceptor concentration dependence of energy-transfer rate obtained experimentally in Eq. (1). In the fit, a is treated as a fitting parameter and the value of k_r used corresponds to that for the porous Si without iodine molecules. R_0 is given in angstrom,²²

$$R_0 = 0.211[\kappa^2 n^{-4} Q_0 J(\lambda)]^{1/6}, \quad (2)$$

where κ is a factor describing the relative orientation in space of the dipoles of the donor and acceptor. Q_0 is the quantum yield of donor in the absence of acceptor. n is the refractive index of the medium. $J(\lambda)$ is the overlap integral given by the spectral overlap between the donor emission and the acceptor absorption. In the calculation of R_0 , κ^2 is assumed to be $2/3$, which is the value for a random distribution of interacting dipoles,²² n is assumed to be 1.48, and $J(\lambda)$ is calculated from our experimental spectra (Fig. 1). We assume Q_0 to be unity because an individual nanocrystalline Si has a large PL quantum efficiency²⁵ although the value for an assembled nanocrystalline Si was reported to be several percent.²⁶

Figure 6 shows the energy-transfer rate detected at 650 nm as a function of iodine concentration. Closed squares and solid line represent the experimental data and fitting result of using Eq. (1) at the donor-acceptor closest approach distance $a=0.45$ nm. Good agreement between the calculation and experiments is obtained in spite of the simple assumption for the calculation. The good agreement indicates that the energy transfer between excitons and iodine molecules is caused by the Förster-type dipole-dipole interaction.

The rate of Förster-type energy transfer strongly depends on the oscillator strength of donor and spectral overlap between PL of donor and absorption of acceptor. Therefore, the origin of the emitted wavelength dependence of energy-transfer rate in Fig. 5(b) can be explained as follows: the increase in the energy-transfer rate in shorter wavelength region results from two factors. First is the larger spectral overlap between PL of porous Si and absorption of iodine in longer wavelength region. Second is the dependence of the radiative recombination rate on the size of Si nanocrystals. By decreasing the size of Si nanocrystals the oscillator

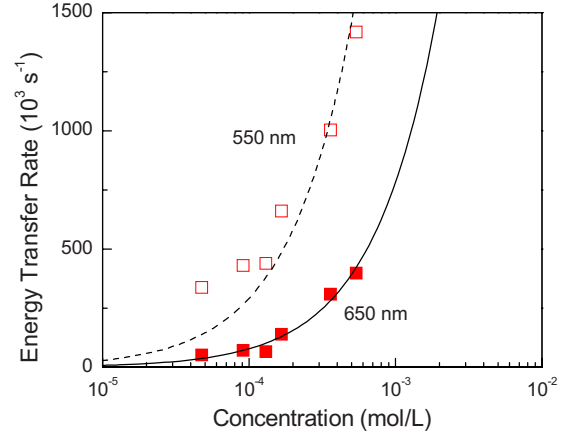


FIG. 6. (Color online) Energy-transfer rate detected at 550 (open squares) and 650 nm (closed squares) as a function of iodine concentration. Dashed and solid lines represent theoretical curves calculated from Eq. (1) for $R_0=2.18$ nm and $a=0.45$ nm.

strength is increased due to the quantum confinement effect, and then the radiative recombination rate is enhanced as shown in Fig. 5(a). The enhancement of the rate results in the increase in the energy-transfer rate.

As shown in Fig. 5(b), the energy transfer depends not only on the emission wavelength but also on the iodine concentration, i.e., at the low iodine concentration the energy transfer in the range from 600 to 800 nm cannot be observed in spite of the spectral overlap, while at the high iodine concentration the nonresonant energy transfer is observed. The nonexistence of energy transfer in the range of 600 to 800 nm at the low concentration may be due to a large mean distance between the iodine species and Si nanocrystals. Although there is a small spectral overlap as seen in Fig. 1, the energy-transfer rate depends not only on the degree of the spectral overlap but also on a distance between the donor and acceptor. At the low concentration the mean distance between the donor and acceptor is relatively large and then the large distance may result in the smearing of energy transfer. On the other hand, the nonresonant energy transfer at the high iodine concentration is due to a smaller distance between the iodine and Si nanocrystals. Although the spectral overlap is smaller than the resonant condition case, the smaller separation at the high iodine concentration allows transfer of the donor energy to the acceptor via dipole-dipole interaction.

It should be noted that disagreement between the calculation and experimental data is observed in the shorter wavelength region. The experimental (open square) and calculated (dashed line) energy-transfer rates at 550 nm are shown in Fig. 6. We can see the deviation at the smaller iodine concentrations. This is probably due to breaking of the assumption that there is an attainment of the rapid-diffusion limit. To satisfy the rapid-diffusion limit, the condition $D\tau/s^2 \gg 1$ is required, where D , s , and τ are the diffusion coefficient, mean distance between donor and acceptor, and lifetime of donor.²⁴ As shown in Fig. 5(a), the porous Si emitted at around 650 nm has relatively longer lifetime, while with decreasing the size of porous Si its lifetime is decreased. With decreasing the lifetime the mean distance diffused by the

porous Si and iodine is comparative to the diffusion distance during the lifetime ($D\tau/s^2 \sim 1$). Then, the rapid-diffusion limit is not attained, resulting in the deviation between the experiment and calculation.

IV. CONCLUSION

The energy transfer from excitons in Si nanocrystals to iodine molecules was studied by using the time-resolved PL spectroscopy. The shortening of the lifetime due to the non-radiative energy transfer was observed and the degree of the shortening depended on the emission wavelength. The energy-transfer rates were increased with increasing the emission wavelength. These results imply that the efficient energy transfer takes place under the resonant condition

where the spectral overlap between the PL of porous Si and the absorption of iodine molecules and the radiative recombination rate of porous Si are large. Furthermore the energy-transfer rates depended on the iodine concentration. The dependence was well explained by the Förster model in which the diffusion of the porous Si powder and iodine molecules is taken into consideration. The present result suggests that the porous Si can be acted as a donor in the energy transfer via dipole-dipole interaction.

ACKNOWLEDGMENTS

This work was supported by a Grant-in-Aid for Scientific Research from the Japan Society for the Promotion of Science and Hosokawa Powder Technology Foundation.

*Author to whom correspondence should be addressed.
nakamura@el.gunma-u.ac.jp

¹L. T. Canham, Appl. Phys. Lett. **57**, 1046 (1990).

²C. Delerue, M. Lannoo, G. Allan, and E. Martin, Thin Solid Films **255**, 27 (1995).

³D. Kovalev, H. Heckler, G. Polisski, and F. Koch, Phys. Status Solidi B **215**, 871 (1999).

⁴A. G. Cullis, L. T. Canham, and D. J. Calcott, J. Appl. Phys. **82**, 909 (1997).

⁵B. Gelloz, A. Kojima, and N. Koshida, Appl. Phys. Lett. **87**, 031107 (2005).

⁶A. J. Kenyon, P. F. Trwoga, M. Federighi, and C. W. Pitt, J. Phys.: Condens. Matter **6**, L319 (1994).

⁷M. Fujii, M. Yoshida, S. Hayashi, and K. Yamamoto, J. Appl. Phys. **84**, 4525 (1998).

⁸D. Kovalev, E. Gross, N. Künzner, F. Koch, V. Y. Timoshenko, and M. Fujii, Phys. Rev. Lett. **89**, 137401 (2002).

⁹B. Goller, S. Polisski, and D. Kovalev, Phys. Rev. B **75**, 073403 (2007).

¹⁰N. J. Turro, *Modern Molecular Photochemistry* (University Science Books, Sausalito, CA, 1991).

¹¹I. L. Medintz, A. R. Clapp, H. Mattoussi, E. R. Goldman, B. Fisher, and J. M. Mauro, Nature Mater. **2**, 630 (2003).

¹²S. A. Crooker, J. A. Hollingsworth, S. Tretiak, and V. I. Klimov, Phys. Rev. Lett. **89**, 186802 (2002).

¹³V. A. Karavanskii, A. A. Chistyakov, G. E. Kotokovskii, M. B. Kuznetsov, and K. V. Zakharchenko, Phys. Status Solidi B **197**, 403 (2003).

¹⁴S. Limaye, S. Subramanian, B. Goller, J. Diener, and D. Kovalev, Phys. Status Solidi A **204**, 1297 (2007).

¹⁵J. Tellinghuisen, J. Chem. Phys. **58**, 2821 (1973).

¹⁶H. Okabe, *Photochemistry of Small Molecules* (Wiley, New York, 1978).

¹⁷A. Fojtik and A. Henglein, Chem. Phys. Lett. **221**, 363 (1994).

¹⁸J. K. M. Chun, A. B. Bocarsly, T. R. Cottrell, J. B. Benziger, and J. C. Yee, J. Am. Chem. Soc. **115**, 3024 (1993).

¹⁹A. Fojtik and A. Henglein, J. Phys. Chem. B **110**, 1994 (2006).

²⁰M. Fujii, D. Kovalev, B. Goller, S. Minobe, S. Hayashi, and V. Y. Timoshenko, Phys. Rev. B **72**, 165321 (2005).

²¹T. Takagahara and K. Takeda, Phys. Rev. B **46**, 15578 (1992).

²²J. R. Lakowicz, *Principles of Fluorescence Spectroscopy* (Springer, New York, 2006).

²³Y. Elkana, J. Feitelson, and E. Katchalski, J. Chem. Phys. **48**, 2399 (1968).

²⁴D. D. Thomas, W. F. Carlsen, and L. Stryer, Proc. Natl. Acad. Sci. U.S.A. **75**, 5746 (1978).

²⁵S. Miura, T. Nakamura, M. Fujii, M. Inui, and S. Hayashi, Phys. Rev. B **73**, 245333 (2006).

²⁶W. L. Wilson, P. F. Szajowski, and L. E. Brus, Science **262**, 1242 (1993).